An In-Silico Study of the Effects of Conductance Variation on the Regionally Based Action Potential Morphology

Jordan Elliott[1], Olaf Dössel[2], Axel Loewe[2], Luca Mainardi[1], Valentina Corino[1], José Felix Rodriguez Matas[1]

[1]Politecnico Di Milano, Milan, Italy [2]Karlsruher Institut für Technologie, Karlsruhe, Germany

Abstract

Improved understanding of the effects of variability in electrophysiological activity within the human heart is key to understanding and predicting cardiovascular response to disease and treatments. Previous studies have considered either regional variation in action potentials or inter-subject variability within a single region of the atria. In this study, we hypothesize that the regional differences in morphology derive not only from variation in dependence on individual conductances, but also from the relationship between multiple conductances.

Using the Monte-Carlo Sampling Method and the Maleckar cellular model for electrophysiology, we created an in-silico population of models. Each conductance was varied +/- 100% from the standard model. The population was divided into regional groups based on biomarkers.

Results showed regional variation in the dependence on relationships between conductances. In the right atrial appendage the value of gK1 was found to be only twice as influential as the relationship between gK1 and gKur on the APD90 biomarker. Other relationships that had a significant impact included gTo-gKur; gKr-gK1; gNaK-gNaCa and gKur-gNaK for various regions. R^2 values for first order linear regression models showed significant relationships were left out in the analysis. This was significantly improved in the second order R^2 values.

1. Introduction

Variability in cellular electrophysiology is an important consideration when modelling and understanding the behaviour of the heart. Despite this, the cellular models used to date typically only consider the average experimental recordings from populations, ignoring variability due to its complexity. Some studies have introduced the use of a population of models to introduce cellular variability [1][6][7], whereas other studies introduce regional variability without including cellular variability [2-5]. This study aims to present the effects of combining regional and cellular variability and the importance of considering both when modelling the atrial response to stimulus.

Several studies have been undertaken in an attempt to characterise the action potential (AP) morphology of various atrial regions in both humans and canines [1][2][4][7], however due to the limitations in collecting this data, a complete regional classification of the human atria AP morphology does not currently exist. As a result, supplementing available human based data with that of canine observations is standard practice [4][5].

In this study we create a regionally based population of models using the Maleckar model and a combination of human and canine based AP morphology data to calibrate the regional populations with varying conductance densities. The experimentally calibrated regional populations are used to analyse the individual contribution of ionic currents and the contributions of specific combinations of currents.

By calibrating the regional populations using AP morphology and specified biomarkers, each population consists of an unbias combination of conductance values. Observing the resulting population dynamics enables a regional based evaluation of the significance of each ionic conductance and relationships between different ionic currents.

2. Methodology

2.1. Population of Models

A total of 9 conductances were varied with +/- 100% from the original maximum value given in the Maleckar model [8]. These were the ultra rapid, rapid, slow, transient outward and inward rectifier potassium currents (I_{Kur}, I_{Kr}, I_{Ks}, I_{To} and I_{K1} respectively), the fast sodium current (I_{Na}), the L-type calcium current (I_{CaL}), the sodium/potassium pump (I_{NaK}) and the sodium calcium exchanger (I_{NaCa}).

A population of models was created using the Maleckar model for the action potential of an atrial cell. After preconditioning, each subject was stimulated at 1Hz, 45pA/pF with a stimulation duration of 1.0ms.

	AVR	RA	RAA	LA	LAA	CTBB	PM
APD90	280 +/- 28.6	336 +/- 30.8	318 +/- 21.9	300 +/- 33.7	288 +/- 21.9	330 +/- 64.0	296 +/- 19.2
APD50	58 +/- 21.4	106 +/- 36.8	139 +/- 36.0	85 +/- 16.7	126 +/- 12.8	185 +/- 32.0	115 +/- 16.5
APD20	7 +/- 6.6	7 +/- 6.6	7 +/- 6.6	7 +/- 6.6	7 +/- 6.6	7 +/- 6.6	7 +/- 6.6
APA	115 +/- 21.4	105 +/- 13.4	116 +/- 19.2	102 +/- 3.9	120 +/- 19.2	122 +/- 19.2	119 +/- 16.5
RMP	-71 +/- 1.4	-73 +/- 12.0	-76 +/- 6.6	-73 +/- 5.4	-71 +/- 6.6	-75 +/- 1.9	-73 +/- 12.0
Final Population Size	328	570	404	201	264	218	293

Table 1 Showing the mean and standard deviation of each region used for regional classification in the population of models. Regional values for the biomarkers taken from previously published experimental data. The table also shows the final regional population sizes.

Using the Monte Carlo Sampling Method, a population of 13,689 stable subjects was created, of which 1,146 subjects fell within the acceptable range for all biomarkers for at least one atrial region. Unstable subjects were removed from the population.

2.2. Regional classification

The atria were divided into 7 regions: The left and right atria (LA and RA) and their associated appendages (LAA and RAA); the pectinate muscles (PM); the crista terminalis and Bachmanns Bundle (CTBB) and the atrio-ventricular rings (AVR). Using a combination of previously published work [1][3-5][7], each region was assigned a mean and standard deviation for the 5 biomarkers: resting membrane potential (RMP), action potential amplitude (APA), action potential at 20% repolarisation (APD20), 50% repolarisation (APD50), and 90% repolarisation (APD90). Due to the lack of experimental data for various regions of the human heart, this was combined with the available data for the canine heart, scaled based on comparative regions.

The biomarkers for each region are shown in Table 1. Using the population of models, regional datasets were populated using two standard deviations from the target mean for each of the five biomarkers. The final regional population sizes are shown in Table 1.

2.3. Statistical Analysis

Through the use of regression analysis the contribution of each of the 9 varied conductance densities are presented. Regression analysis was also used to identify the relationships between multiple conductance densities and their effect on each of the biomarkers previously identified.

By calculating the R-squared (R^2) coefficient of determination, the ability for the first order and second order regression analysis to capture the behaviour of the population was assessed. The ANOVA test was used to determine the statistical significance of each conductance in relation to the biomarkers, with a p-value of 0.025 or below determining statistical significance.

Boxplots including confidence intervals are used to identify statistical differences in ionic conductance and biomarker between atrial regions, as well as verifying that the population distribution for each region is consistent with the previous experimental data by remaining within one standard deviation of the calibrated mean.

3. Results and Discussion

3.1. Regional population distributions

Figure 1A. shows the mean regional action potential as defined by the mean biomarkers in Table 1. This can be compared with Figure 1B which shows the calculated mean action potential for each regional population. The regional characteristics observed through the population of models is comparable with the expected population characteristics used for calibration.
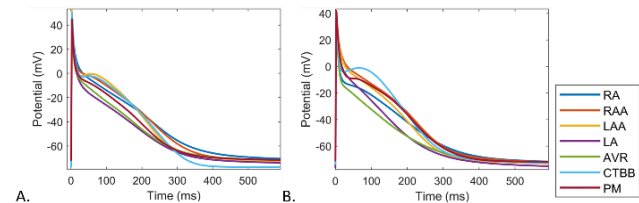

Figure 1 The mean action potential for regional populations. A. shows the mean action potential as calibrated by the experimental data, and B. shows the mean action potential of each regional population.

The unfiltered population consisted of uniform variation in each of the 9 maximum conductances. The overall population, consisting of all action potentials that were included in at least one of the atrial regions, did not show a uniform distribution for the maximum conductances. The distribution for each conductance is shown in Figure 2.

The total population showed great variation in each of the 9 maximum conductances. Figure 3a-3c show the regional distribution of the conductances gKur, gK1 and gCaL. Other conductances, such as gKr, gKs, gTo and gNaCa showed insignificant regional differences.

CTBB has notably the largest range of values, with the distribution showing that gK1 typically exceeds the value

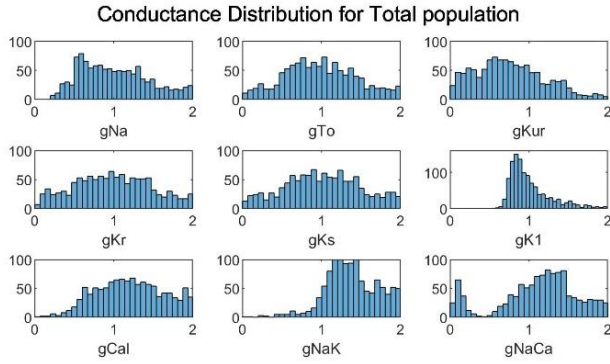Conductance Distribution for Total population

Figure 2 Histograms showing the distribution of the 9 varied conductances for the total population. From left to right the histograms show the distribution of gNa, gTo, gKur, gKr, gKs, gK1, gCaL, gNaK and gNaCa respectively.

set in the Maleckar model. The AVR population shows the opposite for the gK1 conductance, with a significantly smaller range of values and the majority of the population consisting of values below that set in the Maleckar model.

Figure 3d-3f show the variability in the biomarkers APD50, APD90 and APA respectively. The blue 'X' shows the regional mean used for calibration and the green and blue circles show represent the upper and lower boundaries for one standard deviation in each region. Despite slight variation between calibrated mean and observed population mean, for the majority of regions, the population represents the experimental data well. The largest deviation can be seen in the CTBB region, whereby the distribution of both the APD50 and APD90 of the population are significantly lower than the experimental data.

3.2. Linear regression

Overall results from the linear regression showed results consistent with previous studies [1][4][7], whereby the most

significant conductance for APD90 was gK1, with a large negative coefficient across all regions. This was further reflected in the second order linear regression.

For APD90 the inter-conductance relationship between gKur and gK1 had a coefficient of roughly 10% of the coefficient for gK1 alone for all regions. For AVR, PM and RAA the impact was greater, with the gK1-gKur coefficient being 21%, 32% and 51% of the respective gK1 coefficient. This suggests that in RAA the value of gK1 is only twice as influential as the relationship between gK1 and gKur on the APD90. It also shows that the inter-conductive relationship varies greatly between regions. Other relationships that had a significant impact on the APD90 included gTo-gKur for the CTBB, PM and LAA regions; gKr-gK1 for CTBB and LA regions and both gNaK-gNaCa and gKur-gNaK for RAA and CTBB.

APD50 showed similar variation between regions, with the gKr-gK1 relationship being significant only in the LA and PM regions, and gKur-gNaCa being significant only in LAA and PM. Again, moving from first order to second order linear regression, the gK1 conductance changes sign to a large negative coefficient for AVR, CTBB, LA and RA indicating the existance of a significant non-linearity. Once again, this is counteracted through the regional relationship between conductances.

The APD20 biomarker showed similar regional variation, with the three largest relationships being that of gKur with gNaK (LAA, RA, RAA), gKur with gK1 (PM, RAA), and gK3 with gK1 (LA). Once again, regional variations are observed between various conductances.

Tables 2 and 3 shows the associated R^2 values for the first and second order linear regressions respectively. As can be observed, the second order linear regression typically exceeds 0.9. In contrast, the first order linear regression shows far lower R^2 values. This suggests that only considering the individual relationship between maximum conductance and biomarker is insufficient.
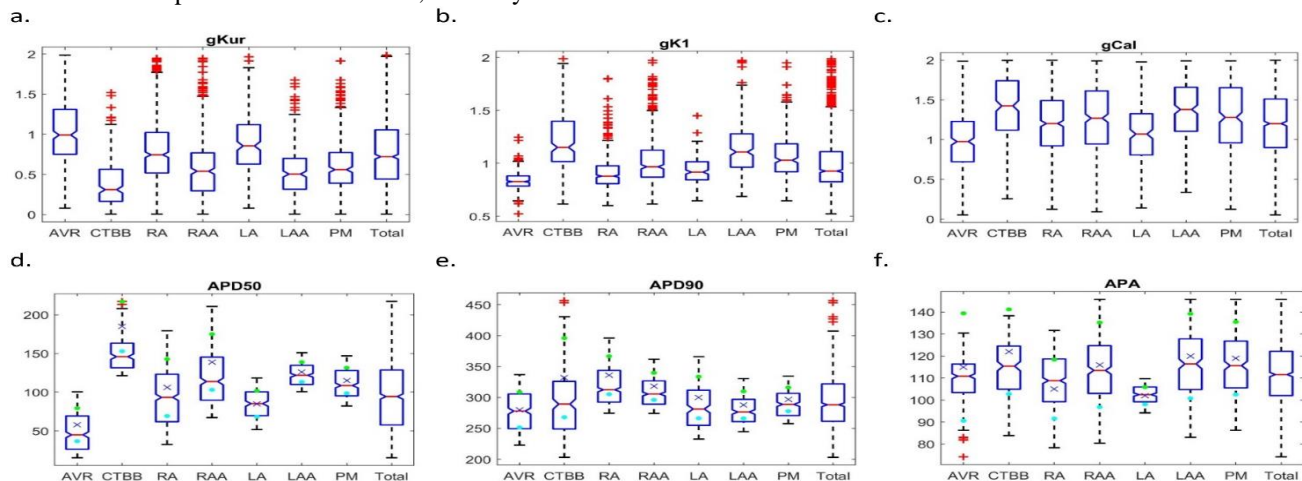

Figure 3 Boxplots showing regional variation of conductances and biomarkers compared with the values used in the standard Maleckar model. a. shows the gKur conductance, b. shows the gK1 conductance, c. shows the gCaL conductance, d. shows APD50, e. shows APD90 and f. shows APA
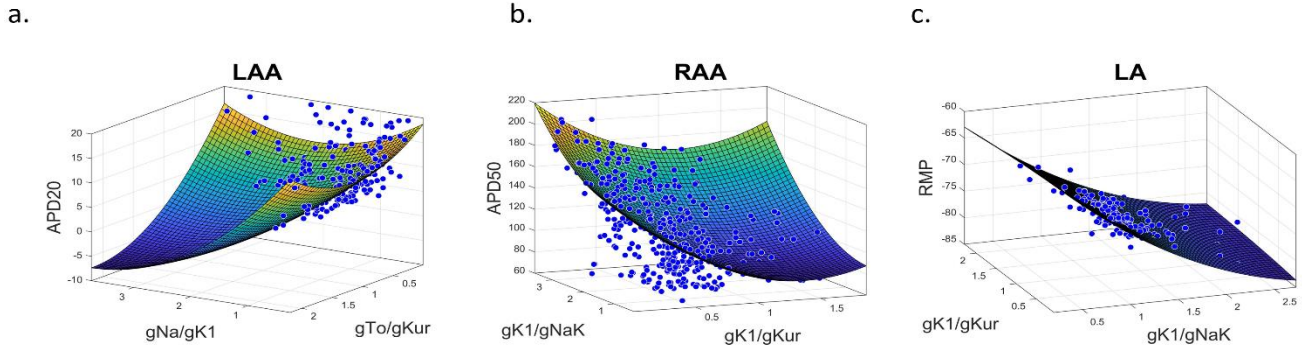
Figure 4 Scatter plots including approximate plane for cross-correlation of multiple maximum conductances with that of the biomarkers. a. shows the correlation with maximum conductances for APD20 for the LAA region, b. shows the RAA region for APD50, and c. shows the LAA region for the RMP.

Table 2 First order linear regression R-squared values

Linear r-square	AVR	CTBB	LA	LAA	PM	RA	RAA	TOT
RMP	0.67	0.68	0.94	0.92	0.94	0.86	0.93	0.86
APA	0.93	0.93	0.57	0.94	0.95	0.9	0.95	0.91
APD20	0.71	0.75	0.8	0.72	0.76	0.72	0.72	0.69
APD50	0.75	0.52	0.76	0.53	0.62	0.82	0.78	0.82
APD90	0.65	0.71	0.81	0.52	0.44	0.41	0.27	0.51

Table 3 Second order linear regression R-squared values

Second order r-square	AVR	CTBB	LA	LAA	PM	RA	RAA	TOT
RMP	0.95	0.94	0.99	0.98	0.99	0.96	0.98	0.95
APA	0.99	0.99	0.97	0.99	0.99	0.97	0.99	0.98
APD20	0.92	0.92	0.97	0.94	0.95	0.92	0.92	0.91
APD50	0.96	0.94	0.94	0.91	0.89	0.93	0.95	0.95
APD90	0.93	0.95	0.97	0.91	0.85	0.84	0.77	0.86

5. Conclusion

This work shows that the action potential morphology is dependent not only on the value of individual maximum conductances, as shown in previous work, but that the relationship between various conductances, such as gKur and gK1 for the APD20 and APD90, also has a significant impact on the action potential. The R^2 values for linear regression clearly show that assuming the different maximum conductances are independent does not accurately represent the relationship with the action potential morphology. In order to represent at least 90% of the dependence and behaviour of the AP morphology, second order linear regression is required. Additionally, this data shows that the dependence on the cross-correlation of conductances varies from region to region.

Further work is to be carried out to determine the effect of cell-to-cell and regional variability in the depolarization and repolarization of the atria through the use of a three-dimensional model. In addition, the effect of pharmacological intervention on the various atrial regions and how this impacts the overall function of the atria would be interesting future work.

Acknowledgments

References

[1]   C. Sánchez *et al.*, "Inter-subject variability in human atrial action potential in sinus rhythm versus chronic atrial fibrillation," *PLoS One*, vol. 9, no. 8, 2014.

[2]   D. Li, L. Zhang, J. Kneller, and S. Nattel, "Potential ionic mechanism for repolarization differences between canine right and left atrium," *Circ. Res.*, vol. 88, no. 11, pp. 1168–1175, 2001.

[3]   H. Zhang, O. Dössel, G. Seemann, F. B. Sachse, A. V Holden, and C. Höper, "Heterogeneous three-dimensional anatomical and electrophysiological model of human atria," *Philos. Trans. R. Soc. A Math. Phys. Eng. Sci.*, vol. 364, no. 1843, pp. 1465–1481, 2006.

[4]   J. Feng, L. Yue, Z. Wang, and S. Nattel, "Ionic mechanisms of regional action potential heterogeneity in the canine right atrium," *Circ. Res.*, vol. 83, no. 5, pp. 541–551, 1998.

[5]   O. V. Aslanidi *et al.*, "3D virtual human atria: A computational platform for studying clinical atrial fibrillation," *Prog. Biophys. Mol. Biol.*, vol. 107, no. 1, pp. 156–168, 2011.

[6]   U. Ravens *et al.*, "Balance between sodium and calcium currents underlying chronic atrial fibrillation termination: An in silico intersubject variability study," *Hear. Rhythm*, vol. 13, no. 12, pp. 2358–2365, 2016.

[7]   X. Liu *et al.*, "From ionic to cellular variability in human atrial myocytes: an integrative computational and experimental study," *Am. J. Physiol. Circ. Physiol.*, vol. 314, no. 5, pp. H895–H916, 2017.

[8]   M. Maleckar *et al.*, " K+ current changes account for the rate dependence of the action potential in the human atrial myocyte ," *Am. J. Physiol. Circ. Physiol.*, vol. 297, no. 4, pp. H1398–H1410, 2009.

Address for correspondence:
Jordan Elliott
LabS, Piazza Leonardo da Vinci, 32, 20133 Milano MI
Jordan.elliott@polimi.it